0026-895X/02/6205-993–1000
MOLECULAR PHARMACOLOGY
U.S. Government work not protected by U.S. copyright
Mol Pharmacol 62:993–1000, 2002

Vol. 62, No. 5
1685/1016928
Printed in U.S.A.

Mice with Partial Deficiency of c-Jun Show Attenuation of Methamphetamine-Induced Neuronal Apoptosis

XIAOLIN DENG, SUBRAMANIAM JAYANTHI, BRUCE LADENHEIM, IRINA N. KRASNOVA, and JEAN LUD CADET

Molecular Neuropsychiatry Section, National Institutes of Health/National Institute on Drug Abuse-Intramural Research Program, Baltimore, Maryland

Received February 21, 2002; accepted July 26, 2002

This article is available online at http://molpharm.aspetjournals.org

ABSTRACT

The regional distribution of c-Jun expression and of the number of apoptotic cells was compared in various brain areas after methamphetamine administration to mice. Our results showed that there was methamphetamine-induced overexpression of c-Jun in the cortex and striatum but not in the cerebellar cortex. There was an almost totally similar regional appearance of methamphetamine-induced apoptotic cells in the mouse brain; no apoptosis was present in the cerebellum. Additionally, in the neocortical area, more positive signals for c-Jun immunoreactivity were observed in the piriform cortex, an area that also showed more positive terminal deoxynucleotidyl transferase-mediated dUTP nick-end labeling (TUNEL) signals than the frontal and parietal cortices. These observations suggested that c-Jun might be involved in methamphetamine-induced apoptosis. This idea was confirmed by using heterozygous c-Jun knockout mice that showed much less apoptosis than wild-type controls. In addition, we found that the majority of TUNEL-positive cells were also positive for c-Jun–like immunoreactivity in both genotypes. Moreover, methamphetamine-induced caspase-3 activity and PARP cleavage were also reduced in c-Jun heterozygous knockout mice. In contrast, methamphetamine-induced hyperthermia was essentially identical in the two genotypes. When taken together, our data support the hypothesis that c-Jun is involved in methamphetamine-induced apoptosis.

METH is a drug of abuse that causes degeneration of monoaminergic nerve terminals and apoptosis (Cadet et al., 1994, 1997; Hirata et al., 1996; Fumagalli et al., 1998; Deng et al., 1999; Deng and Cadet, 2000; see Davidson et al., 2001 for review). METH is thought to cause terminal degeneration via the induction of high body temperature (Bowyer et al., 1992) and of free radicals (Cadet et al., 1994; Hirata et al., 1996; Cadet and Brannock, 1998; LaVoie and Hastings, 1999; Deng and Cadet, 2000). In contrast, the causes of METH-induced cell death in rodent brain are only now beginning to be studied (Stumm et al., 1999; Deng et al., 1999, 2001, 2002; Jayanthi et al., 2001). Other experiments have suggested that superoxide radicals are proapoptotic (Deng and Cadet, 2000), whereas c-Fos might be a protective factor (Deng et al., 1999) in the model of METH-induced cell death. Recently, other lines of evidence have implicated c-Jun in the manifestation of METH-induced neurotoxicity. Specifically, DNA binding experiments had shown some increases in markers of AP-1 activation after METH administration (Sheng et al., 1996). In addition, c-Jun itself and JNK3, which activates c-Jun by phosphorylation at serine 63 and 73 (Kallunki et al., 1996; Herdegen and Waetzig, 2001), are up-regulated in the brain after METH treatment (Cadet et al., 2001; Jayanthi et al., 2001). Putative downstream members of the JNK3-c-Jun gene pathway that are involved in apoptosis, including *p53* and Bax, are also increased after METH treatment (Hirata and Cadet, 1997; Cadet et al., 2001; Jayanthi et al., 2001, Deng et al., 2002).

C-Jun belongs to the family of AP-1 transcription factors, which include Fos and Jun family members. The Jun members can both homodimerize and heterodimerize with other AP-1 members to modulate the expression of some pro-apoptotic genes that contain AP-1 binding sites on their promoter regions (Herdegen and Leah 1998; Shaulian and Karin 2001, Whitfield et al., 2001). This is thought to explain why JNK3 KO mice are resistant to excitotoxicity-induced apoptosis (Yang et al., 1997) and why c-Jun gene mutation (replacement of endogenous Jun by a mutant Jun with serine 63 and 73 mutated to alanines) decreases the hippocampal sensitivity to kainate-induced seizures and neuronal apoptosis (Behrens et al., 1999). Moreover, c-Jun gene KO cells are resistant to apoptosis (Sanchez-Perez and Perona, 1999), whereas transfection of sympathetic neurons with WT c-Jun was shown to induce apoptosis even in the presence of NGF (Ham et al., 1995). Furthermore, death of these cells was prevented by transfecting them with a dominant-negative JNK1 (Eilers

ABBREVIATIONS: METH, methamphetamine; AP-1, activator protein 1; JNK, c-Jun N-terminal kinase; TUNEL, terminal deoxynucleotidyl transferase-mediated dUTP nick-end labeling; WT, wild-type; PARP, poly(ADP-ribose) polymerase; KO, knockout; Ser63 c-Jun, serine 63 phosphorylated c-Jun; Ser73 c-Jun, serine 73 phosphorylated c-Jun.

et al., 1998). When assessed together with our own cDNA array and PCR data (Cadet et al., 2001; Jayanthi et al., 2002), these findings led us to hypothesize that c-Jun might be one of the triggers for METH-induced apoptosis. In the present study, we used c-Jun immunohistochemistry, TUNEL and double-labeling techniques to assess the relationship between cell death and induction of c-Jun in the mouse brain after METH administration. Furthermore, we contrasted the effects of METH on the brains of wild-type and c-Jun+/− mice. Our results confirmed the idea of an involvement of c-Jun in METH-induced apoptosis.

Materials and Methods

Animals and Drug Treatment

Male 10- to 16-week-old (mostly 12-week-old) heterozygous c-Jun KO (c-Jun+/−) as well as C57BL/6J WT (c-Jun+/+) mice, obtained from Jackson Laboratory (JAX MICE, Bar Harbor, ME), were used in these experiments. Homozygous c-Jun KO mice were not used because they die in utero (Johnson et al., 1993). All animal use procedures were according to the National Institutes of Health Guide for the Care and Use of Laboratory Animals and were approved by the local Animal Care Committee.

A single high dose of METH (40 mg/kg), which induces extensive apoptosis in the mouse brain (Deng et al., 2001; Jayanthi et al., 2001), was used in this investigation.

Comparison of c-Jun Expression and Apoptosis in Several Brain Regions of the Mouse

C-Jun Immunohistochemistry. Animal sacrifice and section preparation were performed according to previously reported methods (Deng et al., 1999). Briefly, at 30 min, 2, 4, 8, 16, and 24 h, and 3 days after METH administration, the animals were perfused transcardially, under deep pentobarbital anesthesia with 4% paraformaldehyde. After removal of the brain, 30-μm coronal sections were cut using a cryostat. Free-floating sections were used for c-Jun immunostaining. Sections were first incubated with the c-Jun primary antibody (Cell Signaling, Beverly, MA). Subsequent processing with biotinylated secondary antibody and avidin-biotinylated enzyme complex was performed according to the manufacturer's procedures described in the ABC kit (Vector Laboratories, Burlingame, CA). The free-floating sections were then reacted with 3,3′-diaminobenzidine and hydrogen peroxide to visualize the peroxidase reaction. At the end of the reaction, the sections were mounted on microscope slides for further visualization and analysis. After staining, the number of positive cells were counted (4–5 mice $\times$ 10 sections $\times$ 2 fields of vision/group) under high magnification (40$\times$ objective lens; Carl Zeiss GmbH, Jena, Germany) for statistical analyses.

TUNEL Histochemistry. Another group of C57BL/6J WT mice were used to check the distribution of apoptotic cells in mice brains. Animals were sacrificed 3 days after METH administration. This time point was chosen because our previous studies had shown that there was evidence of increased neuronal apoptosis at this interval after METH injections (Deng et al., 1999). A TUNEL procedure for frozen tissue sections was performed as we described previously (Deng et al., 2001). Briefly, slide-mounted sections from mouse brain were rinsed in 0.5% Triton X-100 in 0.01 M phosphate-buffered saline for 20 min at 80°C to increase permeabilization of the cells. To label damaged nuclei, 50 μl of the TUNEL reaction mixture were added onto each sample in a humidified chamber followed by a 60-min incubation at 37°C. Signal conversion was conducted by adding 50 μl of Converter-POD, then sections were reacted with 3,3′-diaminobenzidine and hydrogen peroxide to visualize the peroxidase reaction. Procedures for negative controls were carried out as described in the manufacture's manual and consisted of not adding the label solution (terminal deoxynucleotidyl transferase) to the TUNEL reaction mixture. No TUNEL-positive cells were observed in the negative controls. For statistical analysis, TUNEL-positive cells in the striatum were counted at each 1 mm^2 using a Zeiss microscope. At least five areas per mouse were measured. Five to seven animals were used in each group for quantification.

Double-Labeling of c-Jun and Apoptosis in the Striatal Cells of Both WT and Heterozygous c-Jun KO Mice

Because it has been reported that activation of c-Jun requires its phosphorylation at serine-63 and -73 (Herdegen and Leah, 1998), we carried out double-label experiments using an antibody against c-Jun phosphorylated at Ser63 in combination with TUNEL staining on sections obtained from the striata of c-Jun+/− mice. We wanted to know the relationship, if any, between c-Jun expression and apoptosis in these cells. Similar approaches have been reported (Garcia et al., 2002). Briefly, 30-μm slide-mounted brain sections were fixed with 4% paraformaldehyde, then incubated with anti-Ser63 c-Jun primary antibody (Cell Signaling). Subsequently they were incubated with biotinylated secondary antibody and Texas Red Avidin DCS (both from Vector Laboratories, Burlingame, CA). After immunostaining, the sections were then processed for TUNEL histochemistry as described above (see *TUNEL Histochemistry* for details).

Comparison of Caspase-3 Activation and PARP Cleavage between WT and Heterozygous c-Jun KO Mice

Caspase-3 Activity Measurement. Caspase-3 enzyme activity was measured in c-Jun+/− and WT mice as described previously (Deng and Cadet, 2000). Briefly, striatal tissues from each group (eight mice) were dissected, then sonicated with lysis buffer containing 25 mM HEPES, pH 7.5, 10 mM dithiothreitol, 10 μg/ml pepstatin, 10 μg/ml leupeptin, and 1 μM phenylmethylsulfonyl fluoride. The lysate was centrifuged for 20 min at 16,000*g*. The supernatant was used for the ApoAlert caspase-3 colorimetric assay (BD Biosciences Clontech Inc., Palo Alto, CA).

PARP Western Blot. Analyses of PARP and its cleavage in the striata of WT and c-Jun+/− mice were performed by Western blot as described previously (Deng and Cadet, 2000). Briefly, dissected tissues were sonicated individually in a 62.5 mM Tris-HCl buffer, pH 6.8, 5 μl/mg tissue, containing 2% SDS and 5% β-mercaptoethanol, then incubated at 90°C for 10 min. Homogenates were centrifuged at 13,000 rpm for 5 min. The supernatant fraction was subjected to protein quantification and adjustment, then glycerol was added to reach a final concentration of 15%. After SDS-polyacrylamide gel electrophoresis (10%), proteins were electrophoretically transferred to a polyvinylidene difluoride membrane, and nonspecific sites were blocked in 5% nonfat dry milk. Membranes were then incubated in the presence of a polyclonal antibody to PARP (Chemicon Inc., Palo Alto, CA) in Tris-buffered saline. PARP antibody binding and chemiluminescence enhancement were performed by using ECL Western blotting analysis system (Amersham Biosciences Inc., Piscataway, NJ). Blots were then stripped for 2 $\times$ 30 min at 50°C (2% SDS, 100 mM β-mercaptoethanol, and 62.5 mM Tris, pH 6.8) and reprobed with an antibody to α-tubulin (Sigma, 1:2000).

Western Blot Analyses of c-Jun, Ser63 c-Jun, Ser73 c-Jun, JNK and Phosphoralated JNK in Mice Striata

We also sought to determine the levels of expression for c-Jun, phosphorylated c-Jun, JNK, and phosphorylated JNK in the two genotypes in response to METH treatments by using Western blot analyses (see *PARP Western Blot* for details). All antibodies were purchased from Cell Signaling.

Temperature Measurement

Hyperthermia has been reported to correlate with dopaminergic neurotoxicity in mice (Bowyer et al., 1992; Fleckenstein et al., 1997). To examine whether differences in hyperthermia might correlate with any differences in the susceptibility of the two genotypes to METH administration, rectal temperature was monitored in WT and c-Jun+/− mice before and 1 h after METH injection (40 mg/kg) according to reported (Fumagalli et al., 1998).

Statistical Analyses

All data are presented as means ± S.E.M. The data were analyzed by analysis of variance followed by Fisher's protected least significant difference test using the program StatView 4.02 (SAS Institute, Cary, NC). Criteria for significance were set at the 0.05 level.

Results

METH Causes Apoptosis and Induces c-Jun Overexpression in the Cortex and Striatum, but Not in the Cerebellum of Mice. The regional expression of apoptotic cells in the mouse brain is presented for animals sacrificed 3 days after METH administration (Figs. 1A-D; 2A-F and Fig. 3). Figure 1 shows TUNEL-positive cells in some c-Jun–dense (striatum) and c-Jun–light brain (cerebellum) regions.

The regional expression of c-Jun immunoreactivity was followed from 30 min to 3 days after METH application. In general, in saline-injected mice, no signal was detectable in the striatum or cerebellum of control mice (Fig. 1, E and F). A few c-Jun–positive signals were found in the cortex (Fig. 2, G, H, I). METH-induced c-Jun expression was observed as early as 30 min after METH administration (data not shown except for the 4-h and 3-day time points; see below). The positive signals were found in the cerebral cortex and striatum but not in the cerebellum. The densest signals were observed at the 4-h time point (Figs. 1G and 2, J, K, L). Subsequently, the signals began to fade away, but obvious c-Jun–positive signals were still noticeable 3 days after METH administration (Figs. 1I and 2, M, N, O). The immunohistochemical data are consistent with data obtained from cDNA array, PCR, and Western blot analyses (Cadet et al., 2001; Jayanthi et al., 2002).

Figure 2 shows TUNEL-positive signals and c-Jun expression in different subregions of the cortex. More c-Jun– and TUNEL-positive signals were found in the piriform cortex than in the frontal and parietal cortex. Figure 3 shows the quantitative data (3 days after METH administration) and the statistics for c-Jun and TUNEL signals in some representative brain regions. There was coordinate expression of c-Jun– and TUNEL-positive cells in the striatum and the cerebral and cerebellar cortices.

METH Causes Less Cell Death in c-Jun+/− Mice. The coincidence of the regional distribution of c-Jun–positive signals and apoptotic cells in the mouse brain had suggested an involvement for c-Jun in METH-induced apoptosis. To further test this idea, we used double labeling of c-Jun and TUNEL to find out whether cells that were TUNEL-positive also showed increased expression of c-Jun phosphorylated at serine 63, because phosphorylation is important to the activity of the protein. Figures 4 and 5 showed that the majority of TUNEL-positive cells (78.0 ± 4.9% in WT; 76.5 ± 3.5% in c-Jun+/− mice) were c-Jun positive (compare Fig. 4, I and H, L and K). More importantly, there were many fewer TUNEL-positive cells in c-Jun+/− than in WT mice (compare Fig. 4, K and H). Figure 5 shows the quantitative rendering of these observations.

C-Jun+/− Mice Showed Less METH-Induced PARP Cleavage and Caspase-3 Activity than WT Animals. PARP cleavage and caspase-3 activation have previously been reported in METH-treated mice (Deng and Cadet, 2000). We thus measured two indices of apoptosis in both WT and c-Jun+/− mice to contrast their responses to the drug. Consistent with the TUNEL staining, caspase-3 activity measurements and PARP Western blot analyses also showed less changes in METH-treated c-Jun+/− mice (Fig. 6).

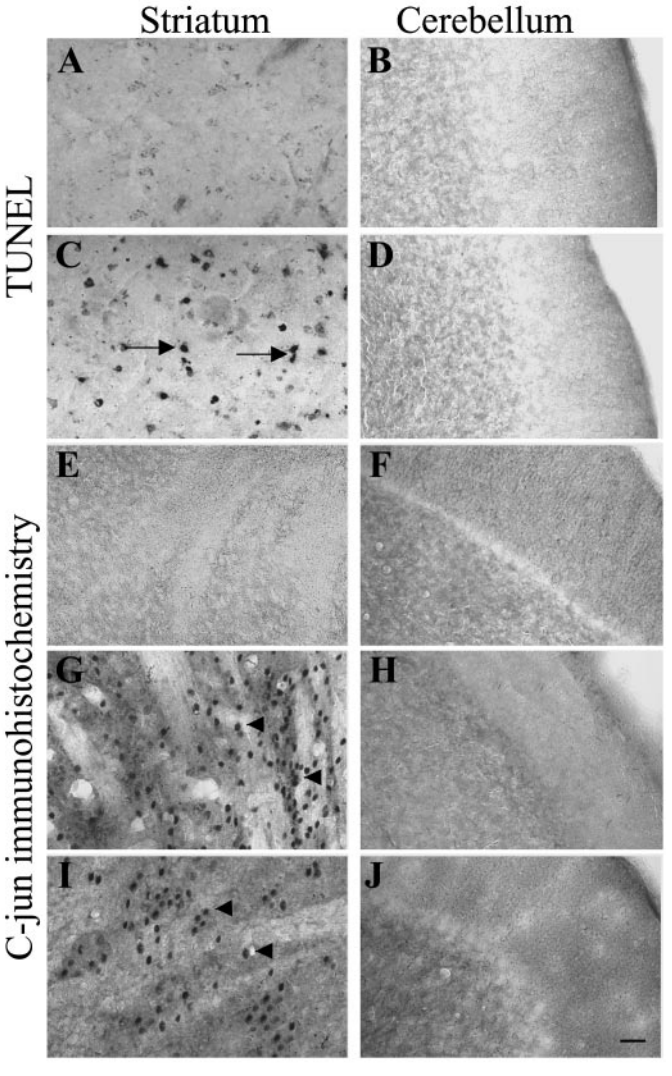

Fig. 1. METH caused apoptosis and increased c-Jun expression in the striatum, but not in the cerebellar cortex of mice. C57BL/6J mice were injected with saline (A, B, E, F) or 40 mg/kg METH (C, D, G, H, I, J) and sacrificed after 4 h (G and H) or 3 days (C, D, I, J). No TUNEL-positive signals were observed in saline-injected mice (A, B). No c-Jun–positive signals were found in the striatum and cerebellum of saline-injected mice (E, F). METH injection caused apoptosis in the striatum (C) but not in the cerebellum (D). In addition, METH administration caused marked increases in the expression of c-Jun in the striatum (G, I) but not in the cerebellar cortex (H, J) of mice sacrificed 4 h and 3 days after METH. Moreover, more c-Jun–positive signals appeared at 4 h than 3 days. Arrows point to TUNEL-positive cells. Arrowheads point to c-Jun–positive signals. Scale bar, 150 μm.

C-Jun+/− Mice Showed Less Induction of c-Jun and of c-Jun Phosphorylated at Ser63 and Ser73, but Similar JNK Induction Compared with WT Mice. The expression of c-Jun, phosphorylated c-Jun, JNK and phosphorylated JNK were also measured and compared between c-Jun+/− and WT mice to contrast the expression of these proteins in the two groups of mice. As shown in Fig. 7, Western blots showed results consistent with those obtained in the immunohistochemical studies. Briefly, METH caused significant increases in both c-Jun and phosphorylated c-Jun. These changes subsequently tapered back toward control levels. In general, the expression of c-Jun in c-Jun+/− mice

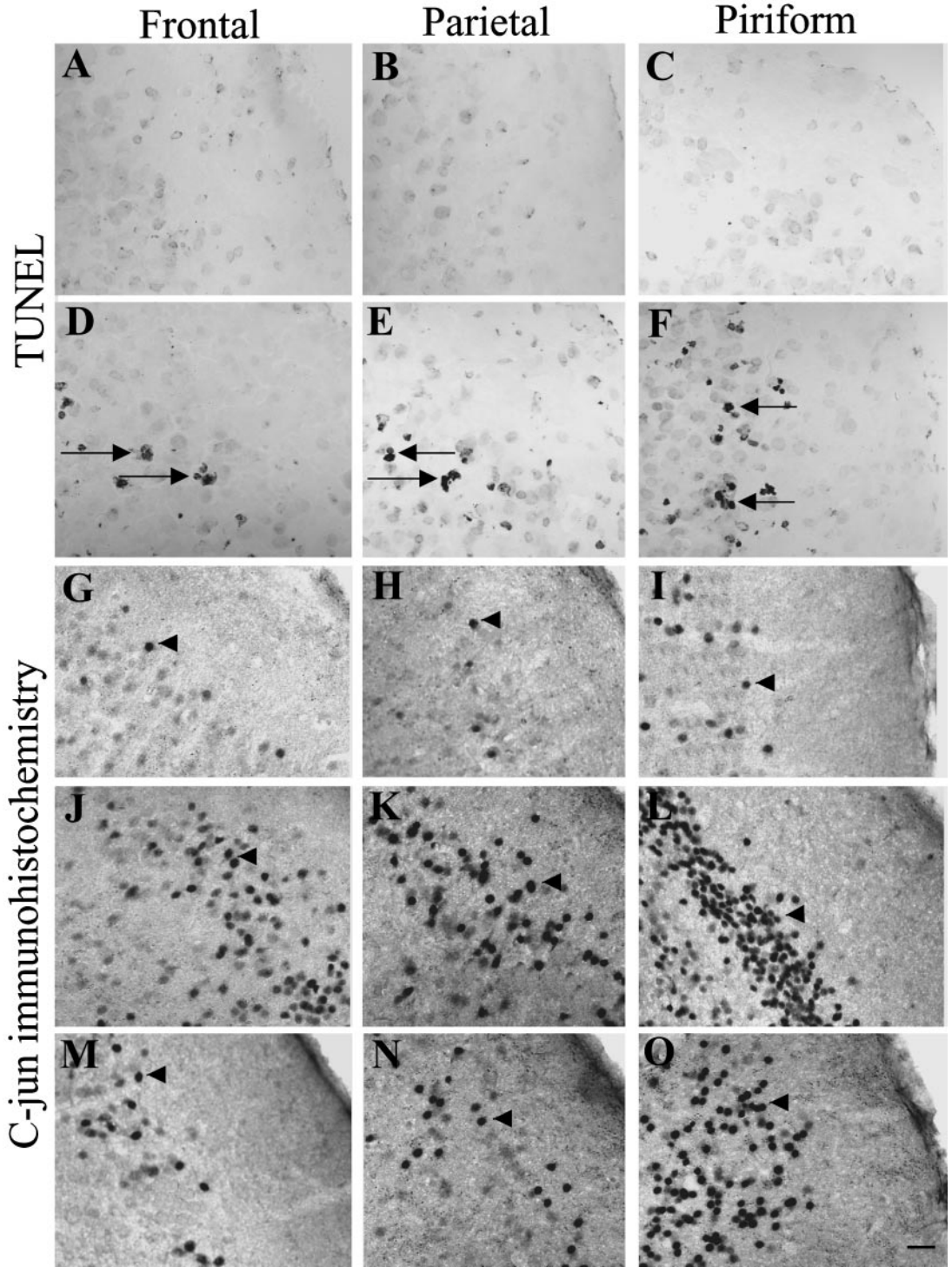

Fig. 2. METH caused a greater number of apoptotic cells and greater c-Jun expression in the piriform than in the frontal and parietal cortex. Sections used for TUNEL staining were obtained 3 days after METH treatment, whereas those for c-Jun staining were obtained in mice sacrificed at 4 h and 3 days after METH administration. No TUNEL-positive signals were demonstrated in cortices of saline-injected mice (A, B, C). Scarce c-Jun–positive signals were found in all cortical areas of saline-injected mice (G, H, I). There were greater changes in c-Jun and TUNEL-positivity in the piriform (F, L, O) than in the frontal (D, J, M) and parietal (E, K, N) cortices after METH treatment. Arrows point to TUNEL-positive cells. Arrowheads point to c-Jun–positive signals. Scale bar, 150 μm. See Fig. 3 for statistical analyses.

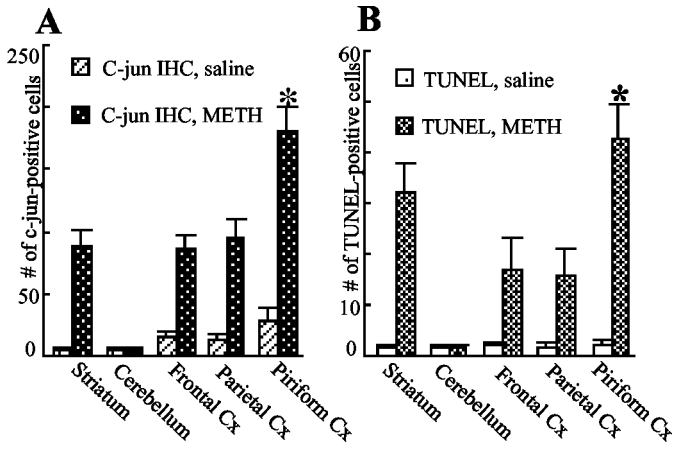

Fig. 3. Quantitative representation of METH effects on the number of TUNEL- and c-Jun–positive cells 3 days after METH treatment. c-Jun expression and TUNEL positive signals were counted in the brain regions listed. The magnitude of METH-induced c-Jun expression is according to the following order: piriform cortex > frontal cortex = parietal cortex = striatum > cerebellar cortex. The order for TUNEL-positive signals in mouse brain is: piriform cortex > frontal cortex = parietal cortex = striatum > cerebellar cortex. *, $p < 0.001$ in comparison to the similar signals in other cortical areas.

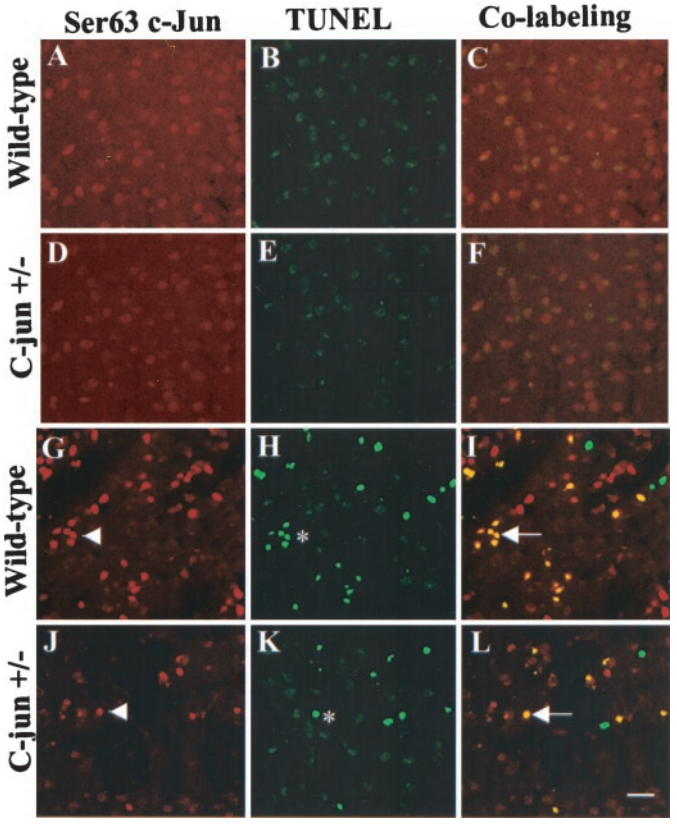

Fig. 4. METH caused less induction of c-Jun and of apoptosis in c-Jun+/− mice. No Ser63 c-Jun–positive (A, D) or TUNEL-positive (B, E) signals were observed in the striatum of control mice. At 3 days after METH administration, both c-Jun–positive (G, J) and TUNEL-positive (H, K) cells were found in the striata of both genotypes. However, fewer positive signals were observed in c-Jun+/− mice compared with WT animals (compare J to G, K to H, L to I). Moreover, double-labeling experiments showed that the majority of TUNEL-positive cells (green) displayed overexpression of c-Jun signals (I, L). Arrowheads point to c-Jun–positive signals (red). Stars represent TUNEL-positive cells. Arrows point to colabeling signals (yellow). TUNEL signals, c-Jun signals, and colabeled signals were counted in a 1-mm^2 striatal area (between Bregma 1.34 to −0.10 mm) respectively. Three sections × three mice were used for the quantitative analyses. The statistical analyses are given in Fig. 5. Scale bar, 150 μm.

was reduced compared with the WT mice at all time points examined. There were no significant differences in JNK and phosphorylated JNK between these two genotypes (Fig. 7). The quantitative results are provided in Fig. 8.

Temperature Fluctuation. Temperature regulation is thought to be important to the manifestations of METH neurotoxicity (Bowyer et al., 1992). Thus, it was possible to suggest that the observed protective effects against METH-induced apoptosis might be because of a lack of hyperthermic responses in these mice. However, we found no differences between the two genotypes in their basal core temperatures (36.9 ± 0.10 and 36.7 ± 0.12 in WT and c-Jun+/−, respectively, $n = 7$). In addition, one h after the injection of 40 mg/kg METH, body temperatures rose to 39.3 ± 0.37 and 39.0 ± 0.44 in WT and c-Jun+/−, respectively (Fig. 9). Thus, it is unlikely that a lack of thermic responses is the cause of the resistance of c-Jun+/− mice to METH-induced apoptosis.

Discussion

Our results showed that the regional distribution of METH-induced c-Jun expression and apoptosis are coincident in the mouse brain. For example, extensive c-Jun protein expression and apoptosis were found in the neocortex and striatum. However, in the cerebellar cortex, neither c-Jun immunoreactivity nor apoptosis was detected after METH administration. These results provide strong correlative evidence that c-Jun may be involved in METH-induced apoptosis. This hypothesis was further confirmed by our use of c-Jun+/− mice, which showed less c-Jun induction, apoptotic cells, caspase-3 activity, and PARP cleavage after METH injection. Moreover, double-labeling experiments showed that about 80% of TUNEL-positive cells showed increased c-Jun expression in both genotypes, indicating that, even in the partial c-Jun deficiency state, c-Jun still played a role in the death of the smaller number of neurons that were killed by METH. In general, our present observations are consistent with those of other investigators who have recently documented an important role for c-Jun in neuronal death caused by various stimuli (Behrens et al., 1999; Whitfield et al., 2001; Garcia et al., 2002). In what follows, we discuss possible scenarios via which c-Jun might participate in METH-induced cell death.

Multiple Pathways Are Involved in METH-Induced Apoptosis in the Mouse Brain. Although METH-induced cell death has been reported by a few laboratories (Schmued

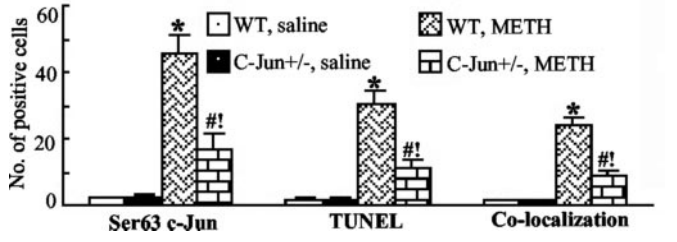

Fig. 5. Quantification of METH-induced changes in Ser63 c-Jun, TUNEL signals and colocalization in the striata of WT and c-Jun+/− mice sacrificed at 3 days after METH treatment. Significantly less positive signals were found in c-Jun+/− than WT mice. Keys to statistics: *, $p < 0.01$ for WT compared with their respective controls; #, $p < 0.01$ for c-Jun+/− compared with their respective controls; !, $p < 0.01$ for comparison between the two genotypes.

and Bowyer, 1997; Eisch et al., 1998; Stumm et al., 1999), the mechanisms for its degenerative effects remain to be clarified. Previous investigations have identified several factors, including high body temperature (Ali et al., 1994), free radicals (Cadet et al., 1995; Cadet and Brannock, 1998), p53 (Hirata and Cadet, 1997), Bcl-2 family proteins (Cadet et al., 1997; Stumm et al., 1999; Jayanthi et al., 2001), and caspase activation (Deng et al., 2002) as possible culprits in METH-induced neurotoxicity. Thus, when taken together with our present observations of an involvement of c-Jun, the accumulated evidence supports the idea that METH-induced apoptosis may result from activation of multiple apoptotic pathways. These pathways may interact with each other to exacerbate METH-induced neurodegeneration. For example, METH-induced free radicals may kill neurons directly (Cadet et al., 1995; Cadet and Brannock, 1998). Free radicals may also do so by increasing the expression of p53 (Ye et al., 1999; Wang et al., 2000), Bax (Kang et al., 1998), or c-Jun (Richter-Landsberg and Vollgraf, 1998; Shukla et al., 2001) via transcription regulation or protein accumulation. Excitatory amino acids released during METH administration (Wallace et al., 2001) may also kill neurons via stimulation of calcium-dependent pathways (Zipfel et al., 2000), c-Jun–dependent mechanisms (Ferrer et al., 1997a,b; Yang et al., 1997), or through activation of mitochondrial death pathway (Montal, 1998; Deng et al., 2002). The effects of the various pathways may also be compounded by METH-induced high body temperature (LaVoie and Hastings, 1999; Fleckenstein et al., 1997). However, temperature regulation does not seem to play a role in the partial protection afforded by the c-Jun+/− genotype because no significant differences in METH-induced hyperthermia were found between WT and c-Jun KO mice. Similarly, the exacerbation of METH-induced apoptosis in c-Fos+/− was not dependent on thermoregulation (Deng et al., 1999). The argument about the existence of multiple triggers for METH-induced cell death might explain, in part, our observations that about 20% of TUNEL-positive cells showed no c-Jun induction in either the WT or c-Jun+/− KO mice (see Fig. 4).

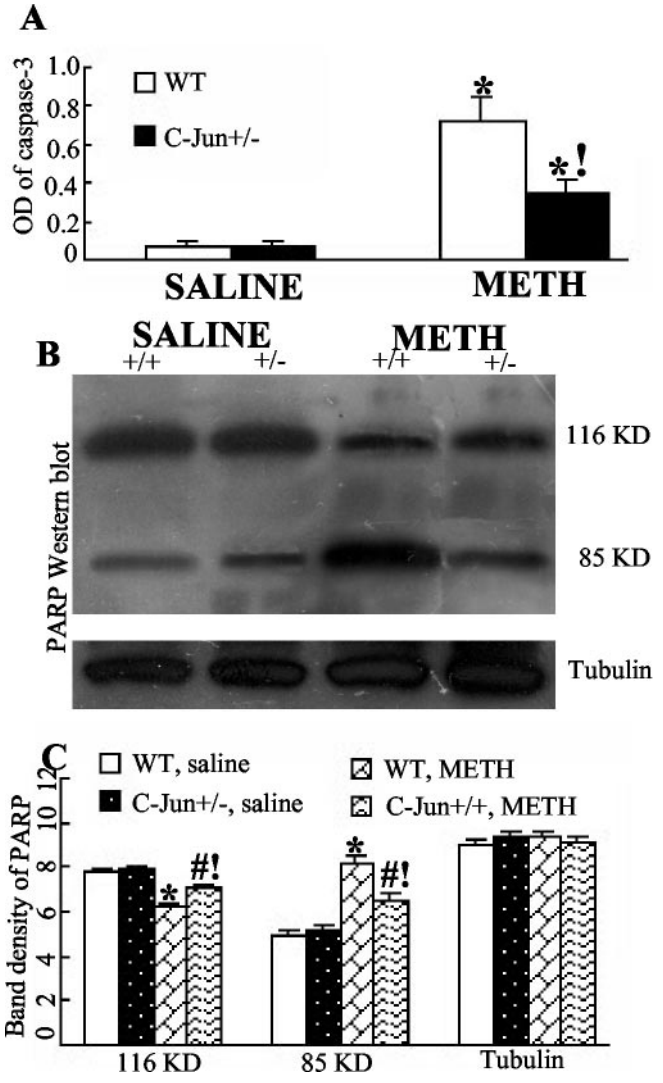

Fig. 6. METH-induced caspase-3 activity (A) and PARP cleavage (B, C) are attenuated in c-Jun+/− mice. Caspase-3 activity measurement and PARP cleavage were conducted according to *Materials and Methods*. A, marked increases in caspase-3 activity were observed after METH injection. *, $p < 0.01$ in comparison with saline-injected mice of similar genotype. There was less increase of caspase-3 activity in c-Jun+/− than in WT mice. !, $p < 0.01$ compared with METH-injected WT mice. B, less PARP cleavage was found in c-Jun+/− mice than in WT mice after METH administration (compare the size of the 85-kDa fragments in lane 3 and lane 4 after METH treatment). C, quantitative representation of PARP cleavage. *, $p < 0.01$ for WT compared with their respective controls; #, $p < 0.01$ for c-Jun+/− compared with their respective controls; !, $p < 0.01$ for comparison between the two genotypes.

The Mode of Action of c-Jun and METH-Induced Cell Death. Homozygous c-Jun KO mice die at mid-gestation (Johnson et al., 1993). This suggests that c-Jun plays important survival roles in utero. In the adult brain, c-Jun is expressed at very low levels; some regions, such as the cerebral cortex or the hippocampus, show higher expression in normal brains (current study; Herdegen and Waetzig, 2001). Environmental stresses of various origins can cause widespread and long-lasting c-Jun overexpression in many brain regions (Ferrer et al., 1997a,b; Garcia et al., 2002). In many cases, this overexpression seems to be linked to cell death (Herdegen and Waetzig, 2001; Garcia et al., 2002). Specifically, JNK3 KO mice are resistant to excitotoxicity-induced apoptosis (Yang et al., 1997), whereas *c-Jun* gene mutation decreases hippocampal sen-

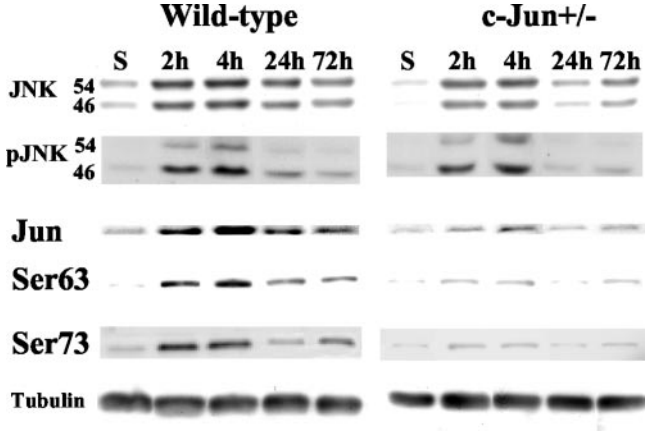

Fig. 7. METH caused no differential JNK expression in WT and c-Jun+/− mice. C-Jun, JNK, and their phophorylated products were analyzed by Western blots in the mice striata. Less c-Jun and phosphorylated c-Jun immunoreactivity was detected in c-Jun+/− mice compared with WT mice. However, no differences in JNK and phosphorylated-JNK were found between the two genotypes. α-Tubulin was also shown and revealed similar loading for all groups. See Fig. 8 for statistic analyses.

sitivity to kainate-induced seizures and neuronal apoptosis (Behrens et al., 1999). Although the pathway that links c-Jun to cell death is not fully understood, the presence of AP-1 binding sites in some proapoptotic proteins, such as cyclin D1, p53, p21, p19, and p16, suggests that c-Jun might have its effects through the regulation of these downstream targets (Herdegen and Waetzig, 2001; Shaulian and Karin, 2001). This suggestion is consistent with the report of METH-induced increases of p53 expression in the striatum (Hirata and Cedet, 1997). P53, in turn, can cause increases in bax and decreases in Bcl-2 (Chiarugi and Ruggiero, 1996; Basu and Haldar, 1998), which may contribute to apoptosis. Increases in Bax and decreases in Bcl-2 have indeed been reported after METH administration, which causes apoptosis in the brain (Jayanthi et al., 2001).

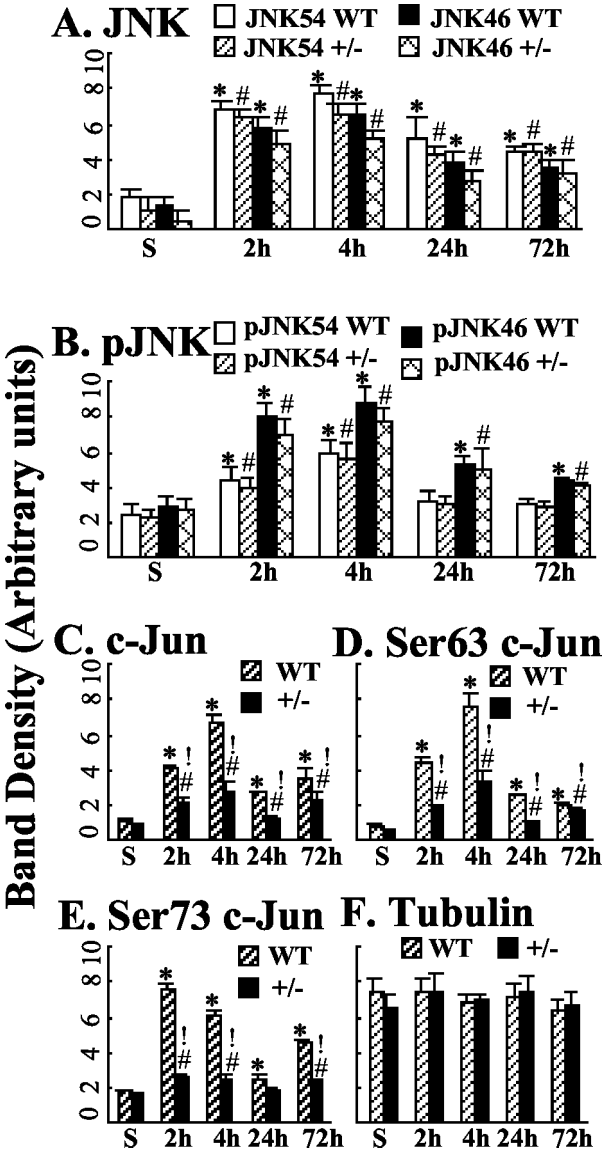

Fig. 8. Quantitative representation of METH-induced effects on c-Jun, JNK, and their phosphorylated proteins. The results are means ± S.E.M. obtained from three experiments (four to six mice of each group). A-F represent JNK, phosphorylated JNK, c-Jun, Ser63 c-Jun, Ser73 c-Jun, and tubulin, respectively. *, $p < 0.01$ for METH-treated animals compared with their respective controls; #, $p < 0.01$ for METH-treated c-Jun+/− compared with their respective controls; !, $p < 0.01$ for between-genotype comparison at a given time point.

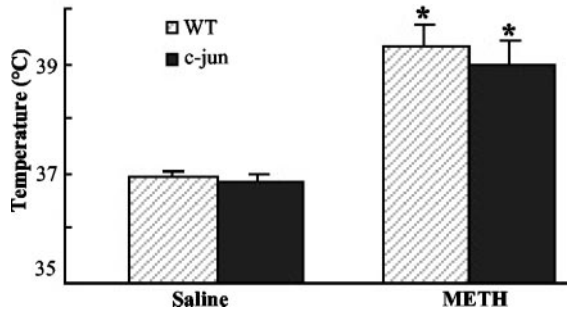

Fig. 9. METH caused similar increases in core temperature in c-Jun+/− and WT mice. WT and c-Jun+/− mice were injected with saline or METH; 1 h later, rectal temperatures were recorded. Marked increases in temperatures were observed after METH treatment. *, $p < 0.01$ for comparison of saline-injected mice of similar genotype.

It is interesting at this point to contrast the present observations with those in our previous article (Deng et al., 1999), in which we reported that c-Fos KO mice were more sensitive to METH-induced apoptosis. When taken together, all these findings provide further evidence for differential functions for c-Fos and c-Jun (Herdegen and Leah, 1998; Herdegen and Waetzig, 2001). It is also interesting to note that the phenotypes of c-Fos and c-Jun KO mice are also quite different (Johnson et al., 1992, 1993). c-Fos–deficient mice showed growth retardation; homozygous mice survived beyond the perinatal period (Johnson et al., 1992), but the homozygous c-Jun KO mice died in utero (Johnson et al., 1993). Thus, c-Jun, but not c-Fos, is essential for life during fetal development. Almost the reverse seems to be true in the case of apoptotic cell death in adulthood because the absence of c-Fos exacerbates (Deng et al., 1999), whereas that of c-Jun protects against apoptosis (present study; see also Behrens et al., 1999; Whitfield et al., 2001; Garcia et al., 2002). These differences might be related to different target genes that, in the case of c-Fos/Jun complexes, might be prosurvival, whereas genes targeted by Jun/Jun complexes might be prodeath during adult life.

Conclusion

In summary, by using c-Jun immunohistochemistry and TUNEL histochemistry, we have reported a substantial degree of coregistration in the regional distribution of c-Jun and apoptosis in the cortex and striatum. Our double-label experiments showed that the majority of TUNEL-positive cells showed increased c-Jun labeling. The observations are similar to those of other investigators (Garcia et al., 2002). It is also important to point out that the percentages of TUNEL-positive cells, in which c-Jun was also induced, are similar between the two genotypes even though less TUNEL-positive signaling, caspase-3 activity, and PARP cleavage were found in c-Jun+/− versus c-Jun+/+ mice treated with METH. Taken together, these observations support the idea that c-Jun–induced mechanisms are involved in METH-induced apoptosis. More studies are needed to further identify the c-Jun downstream targets that participate in the manifestations of

the neurodegenerative effects of this illicit drug. These studies are ongoing in our laboratory.

References

Ali SF, Newport GD, Holson RR, Slikker W Jr, and Bowyer JF (1994) Low environmental temperatures or pharmacologic agents that produce hypothermia decrease methamphetamine neurotoxicity in mice. *Brain Res* **658:**33–38.

Basu A and Haldar S (1998) The relationship between BcI2, *Bax* and p53: consequences for cell cycle progression and cell death. *Mol Hum Reprod* **4:**1099–1109.

Behrens A, Sibilia M, and Wagner EF (1999) Amino-terminal phosphorylation of c-Jun regulates stress-induced apoptosis and cellular proliferation. *Nat Genet* **21:**326–329.

Bowyer JF, Tank AW, Newport GD, Slikker W Jr, Ali SF, and Holson RR (1992) The influence of environmental temperature on the transient effects of methamphetamine on dopamine levels and dopamine release in rat striatum. *J Pharmacol Exp Ther* **260:**817–824.

Cadet JL, Ali SF, Rothman RB, and Epstein CJ (1995) Neurotoxicity, drugs and abuse and the CuZn-superoxide dismutase transgenic mice. *Mol Neurobiol* **11:** 155–163.

Cadet JL and Brannock C (1998) Free radicals and the pathobiology of brain dopamine systems. *Neurochem Int* **32:**117–131.

Cadet JL, Jayanthi S, McCoy MT, Vawter M, and Ladenheim B (2001) Temporal profiling of methamphetamine-induced changes in gene expression in the mouse brain: evidence from cDNA array. *Synapse* **41:**40–48.

Cadet JL, Ordonez SV, and Ordonez JV (1997) Methamphetamine induces apoptosis in immortalized neural cells: protection by the proto-oncogene, bcl-2. *Synapse* **25:**176–184.

Cadet JL, Sheng P, Ali S, Rothman R, Carlson E, and Epstein C (1994) Attenuation of methamphetamine-induced neurotoxicity in copper/zinc superoxide dismutase transgenic mice. *J Neurochem* **62:**380–383.

Chiarugi V and Ruggiero M (1996) Role of three cancer "master genes" p53, bcl2 and c-myc on the apoptotic process. *Tumori* **82:**205–209.

Davidson C, Gow AJ, Lee TH, and Ellinwood EH (2001) Methamphetamine neurotoxicity: necrotic and apoptotic mechanisms and relevance to human abuse and treatment. *Brain Res Brain Res Rev* **36:**1–22.

Deng X and Cadet JL (2000) Methamphetamine-induced apoptosis is attenuated in the striata of copper-zinc superoxide dismutase transgenic mice. *Brain Res Mol Brain Res* **83:**121–124.

Deng X, Cai NS, McCoy MT, Chen W, Trush MA, and Cadet JL (2002) Methamphetamine induces apoptosis in an immortalized rat striatal cell line by activating the mitochondrial cell death pathway. *Neuropharmacology* **42:**837–845.

Deng X, Ladenheim B, Tsao LI, and Cadet JL (1999) Null mutation of c-fos causes exacerbation of methamphetamine-induced neurotoxicity. *J Neurosci* **19:**10107–10115.

Deng X, Wang Y, Chou J, and Cadet JL (2001) Methamphetamine causes widespread apoptosis in the mouse brain: evidence from using an improved TUNEL histochemical method. *Brain Res Mol Brain Res* **93:**64–69.

Eilers A, Whitfield J, Babij C, Rubin LL, and Ham J (1998) Role of the Jun kinase pathway in the regulation of c-Jun expression and apoptosis in sympathetic neurons. *J Neurosci* **18:**1713–1724.

Eisch AJ, Schmued LC, and Marshall JF (1998) Characterizing cortical neuron injury with Fluoro-Jade labeling after a neurotoxic regimen of methamphetamine. *Synapse* **30:**329–333.

Ferrer I, Planas AM, and Pozas E (1997a) Radiation-induced apoptosis in developing rats and kainic acid-induced excitotoxicity in adult rats are associated with distinctive morphological and biochemical c-Jun/AP-1 (N) expression. *Neuroscience* **80:**449–458.

Ferrer I, Pozas E, Ballabriga J, and Planas AM (1997b) Strong c-Jun/AP-1 immunoreactivity is restricted to apoptotic cells following intracerebral ibotenic acid injection in developing rats. *Neurosci Res* **28:**21–31.

Fleckenstein AE, Wilkins DG, Gibb JW, and Hanson GR (1997) Interaction between hyperthermia and oxygen radical formation in the 5-hydroxytryptaminergic response to a single methamphetamine administration. *J Pharmacol Exp Ther* **283:**281–285.

Fumagalli F, Gainetdinov RR, Valenzano KJ, and Caron MG (1998) Role of dopamine transporter in methamphetamine-induced neurotoxicity: evidence from mice lacking the transporter. *J Neurosci* **18:**4861–4869.

Garcia M, Vanhoutte P, Pages C, Besson MJ, Brouillet E, and Caboche J (2002) The mitochondrial toxin 3-nitropropionic acid induces striatal neurodegeneration via a c-Jun N-terminal kinase/c-Jun module. *J Neurosci* **22:**2174–2184.

Ham J, Babij C, Whitfield J, Pfarr CM, Lallemand D, Yaniv M, and Rubin LL (1995) A c-Jun dominant negative mutant protects sympathetic neurons against programmed cell death. *Neuron* **14:**927–939.

Herdegen T and Leah JD (1998) Inducible and constitutive transcription factors in the mammalian nervous system: control of gene expression by Jun, *Fos* and Krox and CREB/ATF proteins. *Brain Res Brain Res Rev* **28:**370–490.

Herdegen T and Waetzig V (2001) AP-1 proteins in the adult brain: facts and fiction about effectors of neuroprotection and neurodegeneration. *Oncogene* **20:**2424–2437.

Hirata H and Cadet JL (1997) p53-knockout mice are protected against the long-term effects of methamphetamine on dopaminergic terminals and cell bodies. *J Neurochem* **69:**780–790.

Hirata H, Ladenheim B, Carlson E, Epstein C, and Cadet JL (1996) Autoradiographic evidence for methamphetamine-induced striatal dopaminergic loss in mouse brain: attenuation in CuZn-superoxide dismutase transgenic mice. *Brain Res* **714:**95–103.

Jayanthi S, Deng X, Bordelon M, McCoy MT, and Cadet JL (2001) Methamphetamine causes differential regulation of pro-death and anti-death Bcl-2 genes in the mouse neocortex. *FASEB J* **15:**1745–1752.

Jayanthi S, McCoy MT, Ladenheim B, and Cadet JL (2002) Methamphetamine causes coordinate regulation of Src, Cas, Crk and the Jun N-terminal kinase-Jun pathway. *Mol Pharmocol* **61:**1124–1131.

Johnson RS, Spiegelman BM, and Papaioannou V (1992) Pleiotropic effects of a null mutation in the c-fos proto-oncogene. *Cell* **71:**577–586.

Johnson RS, van Lingen B, Papaioannou VE, and Spiegelman BM (1993) A null mutation at the c-jun locus causes embryonic lethality and retarded cell growth in culture. *Genes Dev* **7:**1309–1317.

Kallunki T, Deng T, Hibi M, and Karin M (1996) c-Jun can recruit JNK to phosphorylate dimerization partners via specific docking interactions. *Cell* **87:**929–939.

Kang CD, Jang JH, Kim KW, Lee HJ, Jeong CS, Kim CM, Kim SH, and Chung BS (1998) Activation of c-jun N-terminal kinase/stress-activated protein kinase and the decreased ratio of Bcl-2 to Bax are associated with the auto-oxidized dopamine-induced apoptosis in PC12 cells. *Neurosci Lett* **256:**37–40.

LaVoie MJ and Hastings TG (1999) Dopamine quinone formation and protein modification associated with the striatal neurotoxicity of methamphetamine: evidence against a role for extracellular dopamine. *J Neurosci* **19:**1484–1491.

Montal M (1998) Mitochondria, glutamate neurotoxicity and the death cascade. *Biochim Biophys Acta* **1366:**113–126.

Richter-Landsberg C and Vollgraf U (1998) Mode of cell injury and death after hydrogen peroxide exposure in cultured oligodendroglia cells. *Exp Cell Res* **244:** 218–229.

Sanchez-Perez I and Perona R (1999) Lack of c-Jun activity increases survival to cisplatin. *FEBS Lett* **453:**151–158.

Schmued LC and Bowyer JF (1997) Methamphetamine exposure can produce neuronal degeneration in mouse hippocampal remnants. *Brain Res* **759:**135–140.

Shaulian E and Karin M (2001) AP-1 in cell proliferation and survival. *Oncogene* **20:**2390–2400.

Sheng P, Wang XB, Ladenheim B, Epstein C, and Cadet JL (1996) AP-1 DNA-binding activation by methamphetamine involves oxidative stress. *Synapse* **24:** 213–217.

Shukla A, Timblin CR, Hubbard AK, Bravman J, Mossman BT (2001) Silica-induced activation of c-Jun-NH2-terminal amino kinases, protracted expression of the activator protein-1 proto-oncogene, fra-1 and S-phase alterations are mediated via oxidative stress. *Cancer Res* **61:**1791–1795.

Stumm G, Schlegel J, Schafer T, Wurz C, Mennel HD, Krieg JC, and Vedder H (1999) Amphetamines induce apoptosis and regulation of bcl-x splice variants in neocortical neurons. *FASEB J* **13:**1065–1072.

Wallace TL, Vorhees CV, and Gudelsky GA (2001) Effects of lubeluzole on the methamphetamine-induced increase in extracellular glutamate and the long-term depletion of striatal dopamine. *Synapse* **40:**95–101.

Wang S, Leonard SS, Ye J, Ding M, and Shi X (2000) The role of hydroxyl radical as a messenger in Cr(VI)-induced p53 activation. *Am J Physiol* **279:**C868–C875.

Whitfield J, Neame SJ, Paquet L, Bernard O, and Ham J (2001) Dominant-negative c-Jun promotes neuronal survival by reducing BIM expression and inhibiting mitochondrial cytochrome c release. *Neuron* **29:**629–643.

Yang DD, Kuan CY, Whitmarsh AJ, Rincon M, Zheng TS, Davis RJ, Rakic P, and Flavell RA (1997) Absence of excitotoxicity-induced apoptosis in the hippocampus of mice lacking the Jnk3 gene. *Nature (Lond)* **389:**865–870.

Ye J, Wang S, Leonard SS, Sun Y, Butterworth L, Antonini J, Ding M, Rojanasakul Y, Vallyathan V, Castranova V, et al. (1999) Role of reactive oxygen species and p53 in chromium(VI)-induced apoptosis. *J Biol Chem* **274:**34974–34980.

Zipfel GJ, Babcock DJ, Lee JM, and Choi DW (2000) Neuronal apoptosis after CNS injury: the roles of glutamate and calcium. *J Neurotrauma* **17:**857–869.

Address correspondence to: Jean Lud Cadet, M.D., Molecular Neuropsychiatry Section, NIH/NIDA-Intramural Research Program, 5500 Nathan Shock Drive, Baltimore, MD 21224. E-mail: jcadet@intra.nida.nih.gov